CEO Clinical and Experimental Otorhinolaryngology Vol. 15, No. 3: 220-229, August 2022
https://doi.org/10.21053/ceo.2022.00038
pISSN 1976-8710 eISSN 2005-0720

Original Article

Hyaluronan Synthase 1: A Novel Candidate Gene Associated With Late-Onset Non-syndromic Hereditary Hearing Loss

Alphonse Umugire[1,2,*] · Sungsu Lee[1,3,*] · Chang-Joon Lee[4] · Youngmi Choi[1]
Taekyoung Kim[3] · Hyong-Ho Cho[1,3]

[1]Department of Otolaryngology-Head and Neck Surgery, Chonnam National University Hospital, Chonnam National University Medical School, Gwangju; [2]Department of Biomedical Science, College of Medicine, Chonnam National University Graduate School, BK21 PLUS Center for Creative Biomedical Scientists at Chonnam National University, Gwangju; [3]Hospital-based Business Innovation Center, Chonnam National University Hospital, Gwangju; [4]First ENT Clinic, Gwangju, Korea

Objectives. Hyaluronan synthase 1 (HAS1) is a membrane-bound protein that is abundant in the epidermis and dermis, and it is important for skin function. However, its association with hearing loss has not yet been studied. Herein, we sought to evaluate the potential contribution of *HAS1*: c.1082G>A to genetic hearing loss.

Methods. We used whole-exome sequencing to analyze blood DNA samples of six patients of a family with autosomal dominant familial late-onset progressive hearing loss, which was revealed to be related to a variant of the *HAS1* gene. Confirmatory Sanger sequencing was performed with samples from 10 members. A missense variant was detected in *HAS1* (c.1082 G>A, p.Cys361Tyr). *In silico* analyses predicted this variant to result in the functional loss of HAS1. Immunostaining was conducted using wild-type mouse samples to verify HAS1 expression.

Results. Has1 was detected in an otocyst at E10.5. In the pup, Has1 expression was localized in the stria vascularis (SV), hair cells, supporting cells of the organ of Corti, and some spiral ganglion neurons. SV marginal cells markedly expressed Has1 in the adult stage. The hearing threshold in the Has1-depleted condition was investigated by accessing the International Mouse Phenotyping Consortium's Auditory Brainstem Response (ABR) data. ABR of *Has1* knockout mice showed threshold elevations at 6, 12, and 18 kHz in young male adults.

Conclusion. HAS1 may have a close relationship with auditory function and genetic hearing loss. Further investigation is needed to reveal the precise role of HAS1 in the auditory system. *HAS1* is a candidate gene for future hereditary hearing loss genetic testing.

Keywords. *Hyaluronan Synthases; Mutation; Missense; Whole Exome Sequencing; Nonsyndromic Sensorineural Hearing Loss*

INTRODUCTION

Hereditary hearing loss (HHL) is receiving increasing interest owing to recent advancements in next-generation sequencing (NGS). The cost of NGS is continually decreasing, making it possible to evaluate the genetic basis of the condition in increasingly many patients with hearing loss. Thirty percent of HHL cases are syndromic and combined with other symptoms [1], while the remaining 70% are non-syndromic. Among cases of non-syndromic HHL, 80% are autosomal recessive and 20% are autosomal dominant [2]. Autosomal recessive HHL usually pres-

• Received January 5, 2022
Revised March 13, 2022
Accepted March 29, 2022

• Corresponding author: **Hyong-Ho Cho**
Department of Otolaryngology-Head and Neck Surgery, Chonnam National University Hospital, 42 Jebong-ro, Dong-gu, Gwangju 61469, Korea
Tel: +82-62-220-6776, Fax: +82-62-228-7743
E-mail: victocho@hanmail.net

*These authors contributed equally to this work.

ents with hearing loss from the time of birth, resulting in prelingual deafness, whereas autosomal dominant HHL often shows late-onset progressive hearing loss. To date, more than 120 genes have been identified as causing non-syndromic HHL (http://hereditaryhearingloss.org).

Hyaluronan, which is one of the major components of the extracellular matrix, is produced by hyaluronan synthase (HAS). HAS is a membrane-bound protein that is abundant in the epidermis and dermis [3]. Three HAS genes have been identified in humans: *HAS1*, *HAS2*, and *HAS3*. These isoforms have been reported to have different degrees of stability: HAS3 is the most stable protein, HAS2 is less stable, and HAS1 has the least stability [4]. HAS1 is known to be expressed especially in fibroblasts and has important skin functions [3], whereas its expression and function in the auditory organs are largely unknown.

In the present study, we conducted whole-exome sequencing (WES) in a familial case of late-onset progressive severe hearing loss, which was revealed to be related to the *HAS1* gene. We further evaluated the expression and function of HAS1 in the auditory system.

MATERIALS AND METHODS

Participants and clinical evaluation

We evaluated family members of a patient who sought care at a tertiary hospital due to severe hearing loss and received a cochlear implant. A four-generation familial pedigree was obtained. Twelve members of the family (6 affected and 6 unaffected) were subjected to pure tone audiometry and auditory brainstem response (ABR) tests for evaluating their hearing. Peripheral blood samples were collected from 10 of the 12 family members (5 affected and 5 unaffected) for DNA extraction. The study was approved by the Institutional Review Board of Chonnam National University Hospital (IRB No. CNUH-2014-132). All participants provided their informed consent prior to their participation in the study.

DNA isolation from patient blood samples

Genomic DNA was extracted from the patients' peripheral blood using the DNeasy Blood & Tissue kit (Qiagen, Hilden, Germany). DNA quality was verified by agarose gel electrophoresis and DNA quantification was performed by spectrophotometry (NanoDrop 2000; Thermo Fisher Scientific, Waltham, MA, USA).

Exome capture and sequencing

After quality control to ensure the absence of genomic degradation, DNA samples (1 μg) were subjected to library preparation. Libraries with short inserts of 350–450 bp for paired-end reads were prepared using the Truseq DNA Sample Preparation kit (Illumina, San Diego, CA, USA) following the manufacturer's protocol. Whole-exome DNA was sequenced using Illumina HiSeq 4000 at Theragen Etex, South Korea, including an adaptation of the pairwise end-sequencing strategy. In the current study, we performed WES using samples from three affected and three unaffected family members.

Post-sequencing analysis

Burrows-Wheeler aligner (BWA v. 0.6.2) was used to align the sequencing reads, with default parameters, to the Genome Reference Consortium assembly (GRCh37). Alignments were converted from the sequence alignment map format to sorted, indexed binary alignment map files (SAMtools v. 0.1.18). Picard was used to remove duplicate reads. Genome Analysis Toolkit (GATK) software tools (v. 2.3) were used for improving alignments and genotype calling and for refining the default parameters. Genotypes were called using the GATK UnifiedGenotyper, and the GATK VariantRecalibrator tool was used to score variant calls through a machine learning algorithm and to identify a set of high-quality single nucleotide polymorphisms using the Variant Quality Score Recalibration procedure with default parameters. In addition, all variants from both platforms were func-

HIGHLIGHTS

- A point variant (c.1082G>A; p.Cys361Tyr) in *HAS1* was observed in non-syndromic late-onset progressive hearing loss in an autosomal dominant pattern.
- HAS1 is expressed in the otocyst during embryonic development, and its strongest expression occurs in stria vascularis marginal cells in the adult stage.
- *HAS1* may be related to human hereditary hearing loss (HHL) and is a candidate gene for future HHL genetic testing.

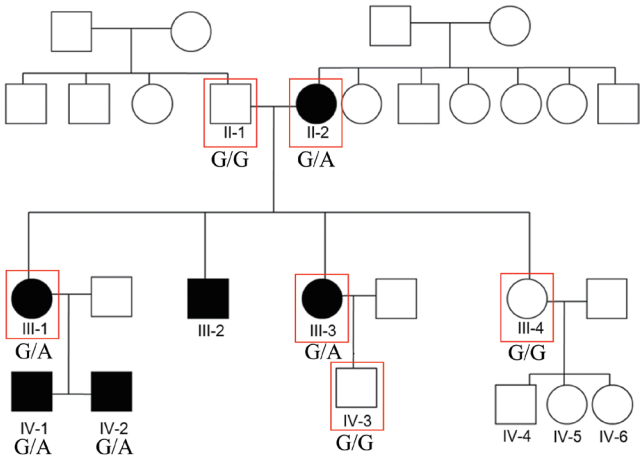

Fig. 1. Familial pedigree of non-syndromic hereditary hearing loss showing an autosomal dominant inheritance pattern. Red boxes indicate participants who were studied by whole-exome sequencing (3 with hearing loss [II-2, III-1, and III-3] and 3 with normal hearing [II-1, III-4, and IV-3]).

tionally annotated using databases from Exome Variant Server (6500). In the last filtering step, markers with GC contents of less than 40% or more than 60% were selected for subsequent downstream analysis.

Validation of variants by Sanger sequencing

Variants for Sanger sequencing validation were randomly selected from the following filters- column filters: pass, ANN impact: moderate, rsID: yes, ExAC: more than average, 1000 Genomes: Caucasian, African high frequency (more than average): filter out, GC_contents: high (maximum) & low (minimum), Korean Center for Disease Control Data Base (KCDCDB) frequency: 0.3–1 homo (10%), hetero (90%, 0/1). Polymerase chain reaction (PCR) primers were designed using Primer 3 software to amplify DNA fragments (ranging in size from 100 bp to 200 bp) with the variants of interest approximately in their center of the sequences. PCR reactions were performed in a 10 μL volume, containing 5 μL of AmpliTaq Gold Fast PCR Master Mix (Applied Biosystems, Foster City, CA, USA), 1.5 μL of each primer at a concentration of 0.5 pmol/μL, and 2 μL of genomic DNA at a concentration of 40 ng/μL. After quality control steps using agarose gel electrophoresis, the product was purified and pooled. Final PCR products were quantified using a Qubit fluorometer (Invitrogen, Carlsbad, CA, USA), and conventional Sanger sequencing was finally performed. First, we conducted NGS and Sanger sequencing with six samples (three unaffected and three affected) resulting in 10 candidate genes as follows: *CHD1, CACNA1B*, *POC1B*,*VEZT*, *LGALS3*, *ZCCHC14*, *BCAM*, *HAS1*,

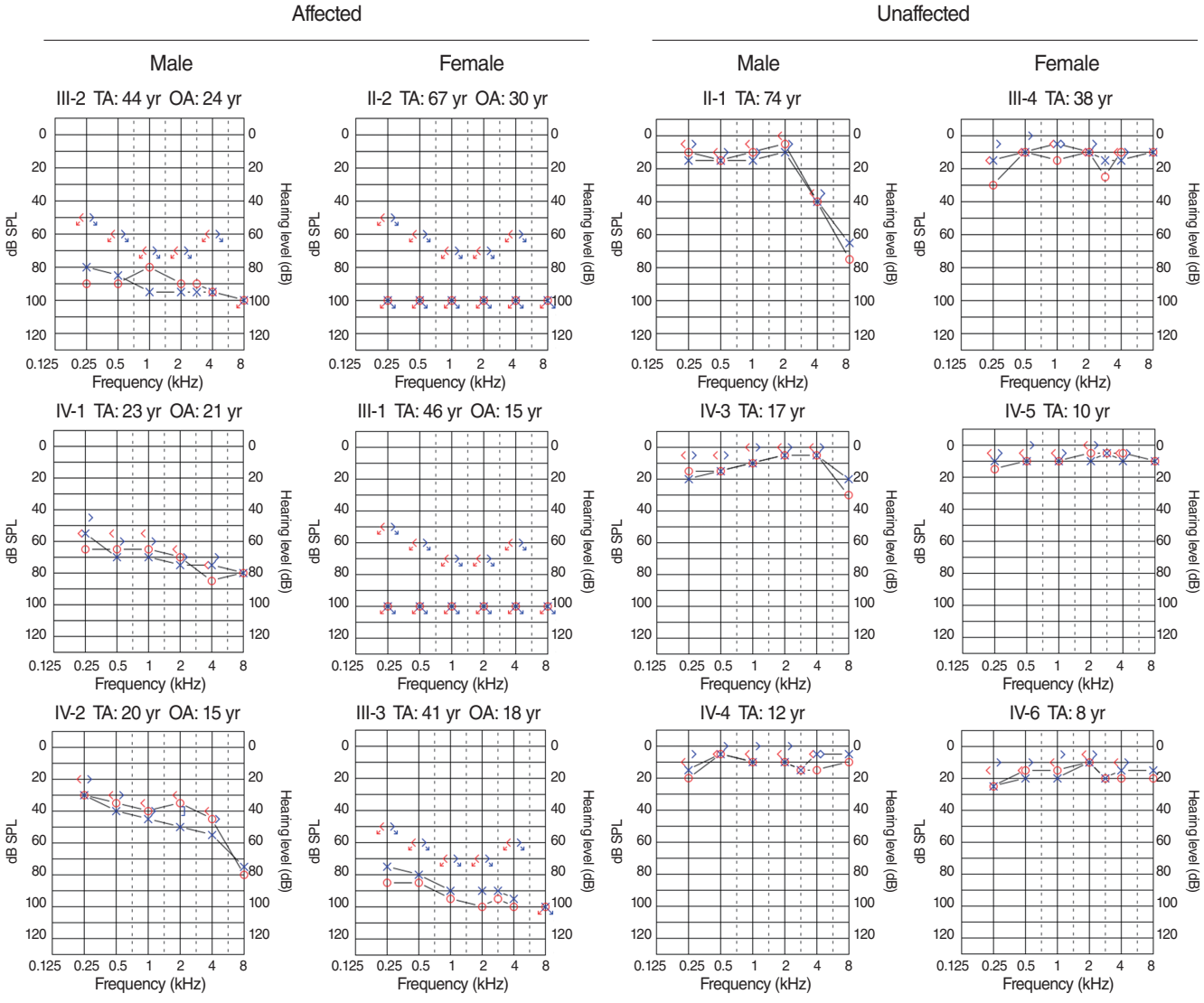

Fig. 2. Pure tone audiometry assessment showing a late-onset progressive severe hearing loss pattern. Hearing loss started in both ears as early as age 15 (patients III-1 and IV-2) and gradually deteriorated afterwards. At age 23, patient IV-1 showed moderate-to-severe hearing loss, and profound deafness occurred around age 40 (III-1, III-2, and III-3). TA, age at audiometry test; OA, age at onset of hearing impairment.

LILRB5, and *KIAA1671*. Then, we further validated these 10 variants including samples of four more family members (two affected and two unaffected). Ten samples (five affected and five unaffected) were evaluated in total, leaving *HAS1* as the final candidate variant gene. We submitted the variant to Leiden Open Variation Database 3 (Variant #0000791276).

Bioinformatic analysis

For variant annotation, we used snpeff 4.1 g. Pathogenicity prediction of variants was performed with Sorting Intolerant from Tolerant (SIFT), Polymorphism Phenotyping v2 (PolyPhen2), MutationTaster and REVEL algorithms by dbNSFP4.2 (http://database.liulab.science/dbNSFP).

Animals and sample preparation, cryosection

We used C57Bl/6 wild type (WT) mice. The number of pregnant female mice (Jax Mice & Services, Bar Harbor, ME, USA) purchased was as required in each embryonic stage timepoint. Mice were euthanized by decapitation under ketamine/xylazine anesthesia. For embryo studies, each sample was washed with phosphate-buffered saline (PBS) and fixed in 2% paraformaldehyde (PFA) at 4°C for 1 hour. Adult mouse cochleae were locally perfused through the round window and further fixed with 4% PFA at room temperature for 2 hours. Then, samples were rinsed with PBS and decalcified with 5% ethylenediaminetetraacetic acid (EDTA) at 4°C for 3–5 days. All samples were embedded in optimal cutting temperature compound (Leica Biosystems, Buffalo Grove, IL, USA) and quickly frozen in dry ice. Sample blocks were sectioned with a Cryostat (Leica CM1850) at 5–20 μm thickness. The animal study was approved by the Chonnam National University Hospital Institutional Animal Care and Use Committee (CNU IACUC-H-2018-42).

Immunostaining

The blocking step was performed in blocking buffer (donkey serum 1:100 in 0.1% PBS-Tween) at room temperature for 1 hour, followed by incubation with the primary antibody at 4°C overnight. After washing, the samples were incubated with secondary antibody (1:1,000 in blocking buffer) at room temperature for 1 hour. Samples were washed thrice with 0.1% PBS-Tween

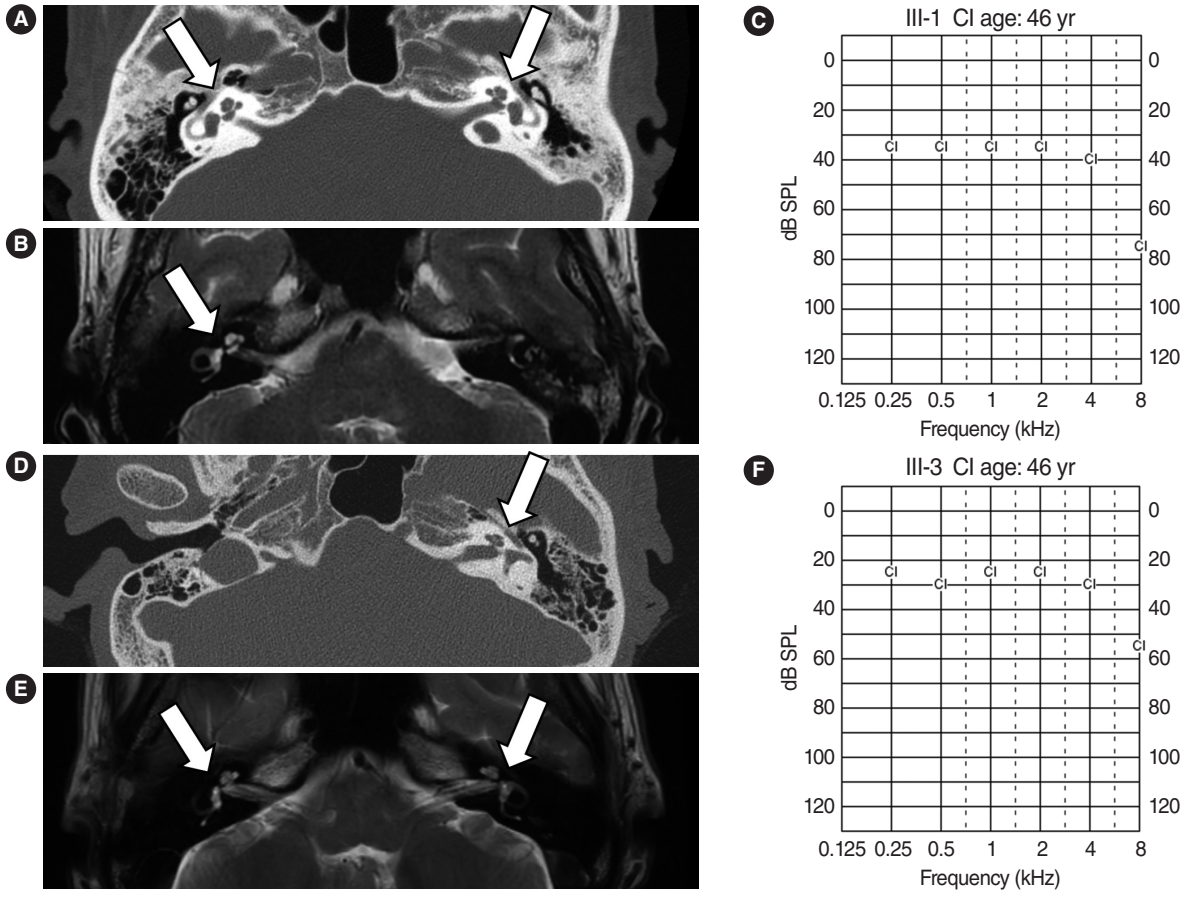

Fig. 3. Normal inner ear anatomy and good outcomes after cochlear implantation (CI) in deaf family members. Temporal bone computed tomography (CT) (A), temporal magnetic resonance imaging (MRI) (B), and postoperative CI-aided pure tone average (PTA; C) results of patient III-1. CT (D), MRI (E), and postoperative CI-aided PTA (F) results of patient III-3. Both patients had no cochleovestibular anomalies (arrows) and showed good hearing performance after CI.

for 30 minutes, stained with 4′,6-diamidino-2-phenylindole (DAPI) for 10 minutes, and were washed with PBS for 30 minutes. Samples were mounted on glass slides with Vectashield (Vector laboratories, Newark, CA, USA) solution and analyzed with an LSM 510 laser scanning microscope (Carl Zeiss Micro Imaging GmbH, Göttingen, Germany). The primary antibodies and titers used in this work were as follows: HAS1 (either goat, 1:200, Santa Cruz Biotechnology #SC-23145, Dallas, TX, USA; or rabbit, 1:200, Abcam #ab198846, Cambridge, UK), HAS2 (rabbit, 1:200, Santa Cruz Biotechnology #SC-66916), HAS3 (goat, 1:200, Santa Cruz Biotechnology #SC-34204), ICAM2 (rat, 1:200, BioLegend #105602, San Diego, CA, USA), Sox2 (rat, 1:200, eBioscience #14-9811-82, San Diego, CA, USA). All secondary antibodies were applied according to the origin of the primary antibody (Jackson ImmunoResearch, Jackson Grove, PA, USA). DAPI (Invitrogen) was used at 1:10,000 titer.

Has1-mutant mice hearing threshold analysis: public data from the International Mouse Phenotyping Consortium

To evaluate the hearing level of mice with depleted Has1, we accessed International Mouse Phenotyping Consortium (IMPC)'s public data (www.mousephenotype.org) [5]. Numbers of mouse ABR data were as follows: Female WT (n=230), Female KO (n=2), Male WT (n=228), Male KO (n=2). ABR data were analyzed with R 4.0.2 using a Wilcoxon rank sum test. The *P*-values below 0.05 were considered statistically significant.

RESULTS

Patterns of inheritance and hearing loss, and cochlear implant outcomes

Hearing impairment affected every generation of the studied family, including both male and female members, showing auto-

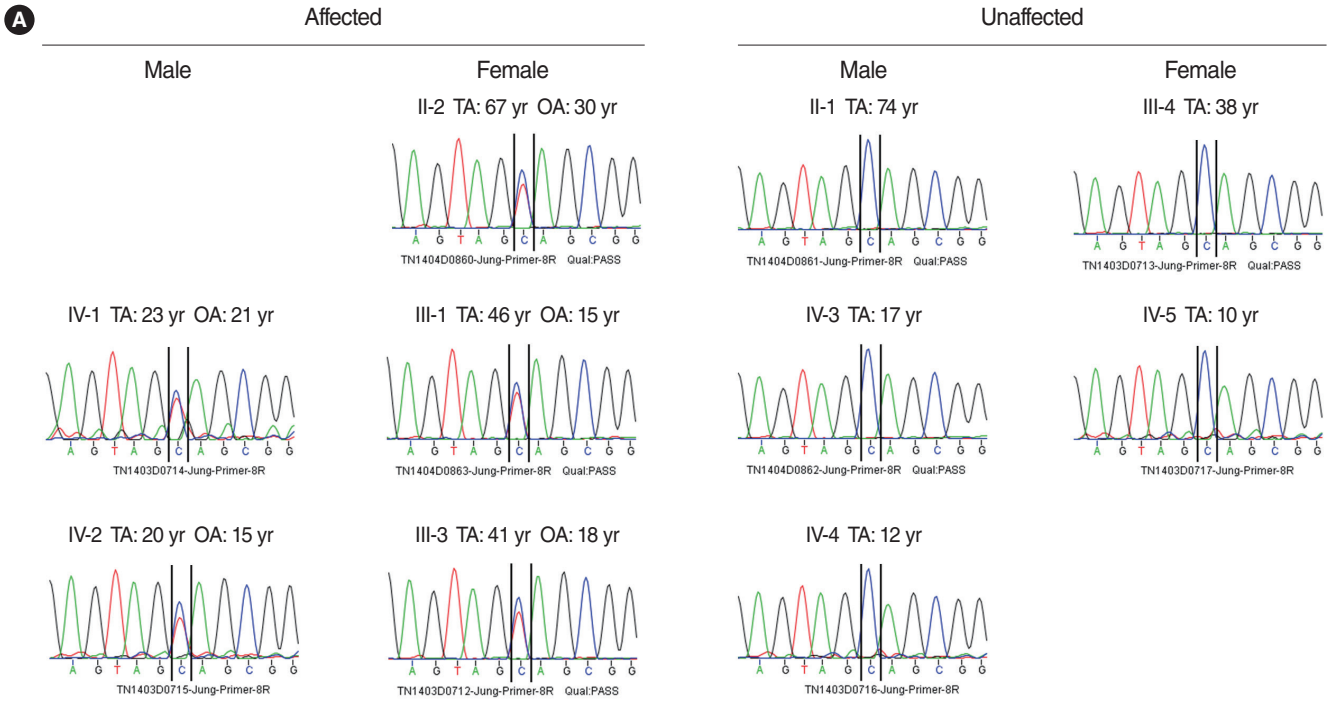

B

A novel variant in the proband of family CNU#15-1				
Gene	NM_num	Position	HGVS_C	HGVS_P
HAS1	NM_001523.3	52217335 chr19	c.1082G>A	p.Cys361Tyr

C

Prediction Information CNU#15-1			
SIFT	PolyPhen2	Mutation Taster	REVEL
Damaging	Damaging	Disease-causing	0.76

Fig. 4. Whole-exome sequencing and Sanger sequencing revealed a missense point variant of *HAS1*. (A) Sanger sequencing confirmed a point variant in hearing-impaired family members. (B) Missense point variant on chromosome 19 in the hyaluronan synthase 1 (*HAS1*) gene (c.1082G>A). (C) "Damaging" and "disease-causing" were the predictions of *in silico* analyses by Sorting Intolerant from Tolerant (SIFT), Polymorphism Phenotyping v2 (PolyPhen2), Mutation Taster, and REVEL. TA, age at audiometry test; OA, age at onset of hearing impairment.

somal dominant inheritance (Fig. 1). None of the family members had other accompanying syndromic phenotypes. The medical history of the affected patients revealed that their hearing was normal from birth until puberty, and they all had normal lingual development. By the age of 15, auditory function started to decrease in both ears. At around age 20, their hearing deteriorated into moderate to severe hearing loss (Two male patients, IV-1 and IV-2) (Fig. 2). At age 40, profound deafness occurred (1 male and 2 female patients, III-1, III-2, III-3). It showed a late-onset progressive severe hearing loss pattern. None of the patients had vestibular symptoms, except for one with non-specific intermittent dizziness (III-3); this patient was also the only one who complained of tinnitus (a buzzing sound). Two female patients underwent cochlear implantation (CI). Preoperative computed tomography and magnetic resonance imaging showed no anatomical anomalies in the cochleae, vestibules, and vestibulocochlear nerves (Fig. 3A, B, D, and E). The CI outcomes were favorable, and the CI-aided pure tone average thresholds were around 30 dB (Fig. 3C and F).

WES and Sanger sequencing revealed a missense variant of *HAS1*

We performed WES using samples from three affected (II-2, III-1, and III-3) and three unaffected (II-1, III-4, and IV-3) participants (Fig. 1). The result showed 10 candidate gene variants (Supplementary Table 1). These results were confirmed with Sanger sequencing using samples from five affected and five unaffected family members (Fig. 4A). Our final results revealed a point variant at chromosome 19, locus 52217335 (Fig. 4B). The gene name was hyaluronan synthase 1 (NM_001523.3), where at position 1,082, guanine was mutated to adenosine (c.1082G>A). Consequently, a cysteine residue was replaced by tyrosine (p.Cys361Tyr). *In silico* analysis was performed using SIFT and PolyPhen2. Both tools predicted that the change should be "damaging" to protein function (Fig. 4C). Another *in silico* analysis by Mutation Taster and REVEL predicted this variant as having "disease-causing" potential (REVEL score 0.76) (Fig. 4C).

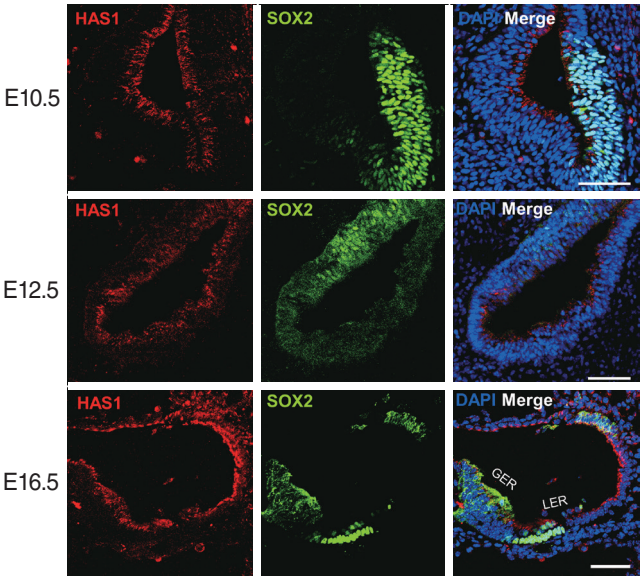

Fig. 5. HAS1 localization in the otic vesicle during mouse embryonic development. HAS1 was already expressed at E10.5 on the apical part of cells lining the luminal surface of the otic vesicle. HAS1 expression continued at E12.5. At E16.5, HAS1 was expressed in the apical membrane of the greater epithelial ridge (GER) region, lateral wall, and hair cells. DAPI, 4′,6-diamidino-2-phenylindole; LER, lesser epithelial ridge. Scale bar: 50 μm.

Has1 is detected during development of the mouse otic vesicle

We evaluated the expression and localization of Has1 in the auditory organs. First, it was evaluated during development in a murine model. At age E10.5, Has1 was detected and localized in the otocyst. The apical membrane of cells lining the lumen robustly expressed Has1 in both the prosensory and non-sensory

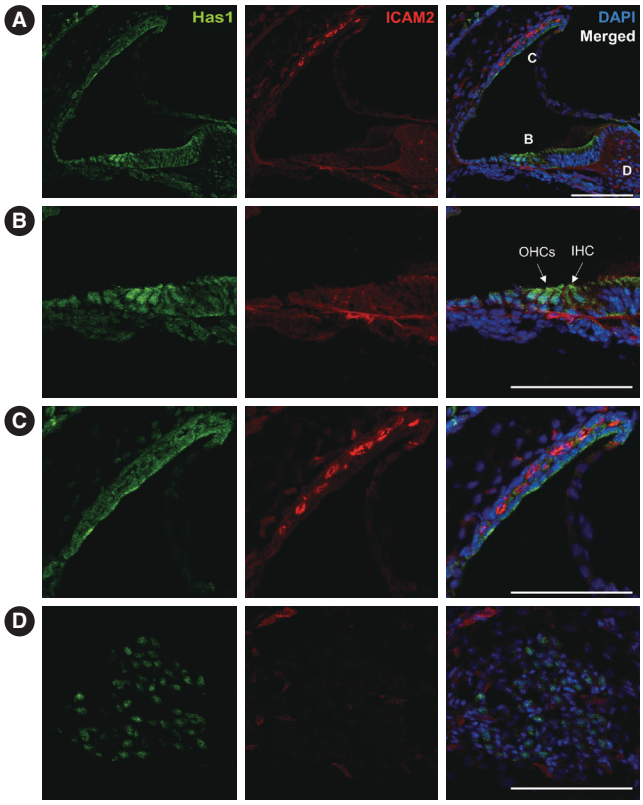

Fig. 6. Has1 expression in neonatal mouse cochlea. (A) Postnatal day 3. Has1 was detected in the cochlea. Intercellular adhesion molecule 2 (ICAM2), an endothelial cell marker, indicates cochlear vessels. (B) Magnified view of the organ of Corti in (A) showing Has1 expression in the inner hair cell (IHC) and outer hair cells (OHCs). Has1 was also weakly expressed in supporting cells and inner sulcus cells. (C) Magnified image of the stria vascularis in (A). The apical membrane of marginal cells showed Has1 expression. (D) Magnified image of the spiral ganglion region in (A). Some spiral ganglion cells also expressed Has1. DAPI, 4′,6-diamidino-2-phenylindole. Scale bar: 100 μm.

regions (Fig. 5). Has1 expression was detected in the cells at E12.5 and E16.5. At E16.5, Has1 localization was observed in the stria vascularis (SV). To date, 3 hyaluronan synthases have been identified: HAS1, HAS2, and HAS3. Unlike Has1, Has2, and Has3 were not detected in the otic vesicle at E14.5 and E16.5 (Supplementary Fig. 1) through immunostaining.

Has1 localization in the SV and organ of Corti after birth

We further checked the expression and localization of this protein in later stages. At postnatal day 3, both inner and outer hair cells of the organ of Corti showed Has1 expression. Supporting cells in the inner and outer sulci also showed weak Has1 expression (Fig. 6A and B). In the lateral wall, Has1 continued to be detected on the apical membrane of SV marginal cells (Fig. 6C). Some spiral ganglion cells also showed Has1 expression (Fig. 6D).

This pattern was maintained in the adult stage, and it was the most robust at the apical membrane of marginal cells in the SV (Fig. 7A and C). Has1 localization signals in the outer and inner hair cells and supporting cells in the organ of Corti were weak compared to those observed in the SV (Fig. 7B). In the vestibular organ, Has1 localization signals were strong in vestibular hair cells and not detected in underlying supporting cells (Supplementary Fig. 2). Has1 localization was observed in some cochlear spiral ganglion cells at the adult stage (Fig. 7D).

Has1 deletion caused low-frequency hearing loss in young adult male mice: IMPC mouse phenotype data

We searched IMPC's public database for the knock-out (KO) phenotype for *Has1* (Fig. 8). The overall click ABR threshold was similar between WT and *Has1*-deleted mice (no significant association, performed in 14-week-old mice). However, interest-

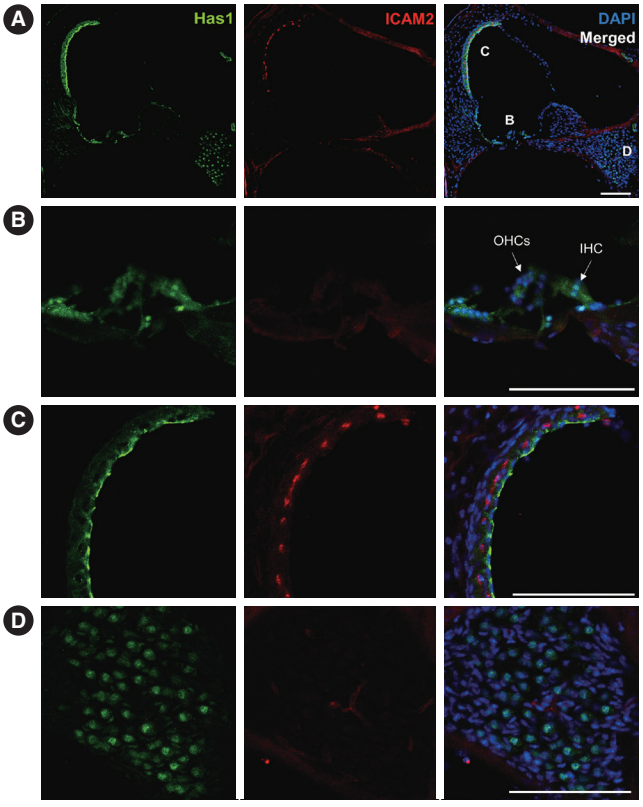

Fig. 7. Has1 expression in adult mouse cochlea. (A) Has1 expression was more confined within the stria vascularis (SV) in 7-week-old mice. (B) Magnified view of the organ of Corti in (A). The expression in hair cells was weaker than in the SV. Hensen's and Claudius cells showed similarly weak expression of Has1. (C) Magnified view of the SV in (A). Has1 was robustly localized in the apical membrane of SV marginal cells. (D) Magnified image of the Rosenthal canal. Has1 was detected in some spiral ganglion cells. ICAM2, intercellular adhesion molecule 2; DAPI, 4′,6-diamidino-2-phenylindole; OHC, outer hair cell; IHC, inner hair cell. Scale bar: 100 μm.

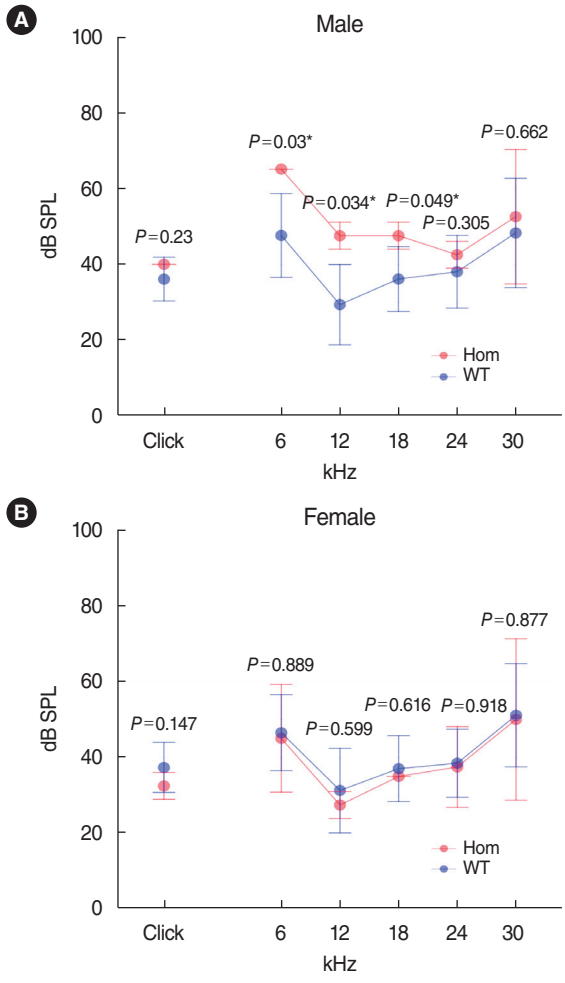

Fig. 8. Hearing threshold elevation in *Has1* knock-out (KO) mice. Hearing levels of 14-week-old *Has1* KO mice. Female *Has1* KO hearing levels were comparable to those of wild-type (WT) mice (female WT: n=230, female KO: n=2). Male *Has1* KO mice showed significant elevations in their hearing thresholds (male WT: n=228, male KO: n=2, $P<0.05$) at 6, 12, and 18 kHz compared to the WT control mice. Public data from International Mouse Phenotyping Consortium (www.mousephenotype.org) were analyzed with R version 4.0.2 (using the Wilcoxon rank sum test). Hom, homozygote. *Statistically significant, $P<0.05$.

ingly, male KO mice showed an elevated ABR threshold at 6 kHz (KO threshold: 65 dB [65–65 dB] vs. WT threshold: 47.6 dB [36.6–58.5 dB]). This threshold was also elevated at 12 kHz (KO threshold: 47.5 dB [44–51 dB] vs. WT threshold: 29.4 [18.9–39.9]). Significant hearing loss was also observed at 18 kHz. The hearing thresholds of female KO mice were comparable to those of WT animals at all frequencies.

DISCUSSION

The family with HHL in this study showed an autosomal dominant trait. To date, 51 genes have been identified as related to autosomal dominant non-syndromic hearing loss (http://hereditaryhearingloss.org). Compared to the autosomal recessive type, which usually presents with severe hearing loss at birth, the autosomal dominant disease shows normal or mild hearing loss during early life [6,7]. Starting from the second decade of life, hearing loss progresses and increases in severity. The family assessed in the current study had a hearing pattern similar to that of previous cases. The earliest recorded onset of hearing loss was in a 15-year-old patient. One affected participant, who was 20 years old, had mild to moderate hearing loss (IV-2) (Fig. 2), and a 23-year-old had moderate to severe hearing loss (IV-1) (Fig. 2). Two family members in their early 40s showed severe hearing loss (III-2 and III-3) (Fig. 2), while one aged 46 years showed complete deafness (III-1). The hearing loss pattern was typical of late-onset progressive severe hearing loss. All participants had normal linguistic development (post-lingual deafness) and did not present with accompanying tinnitus or dizziness, except for one patient. Patient III-3 was a 41-year-old woman with non-specific intermittent dizziness and tinnitus. A hopeful aspect for patients with HHL with this pattern (late-onset progressive HL, post-lingual deafness) is that they experience appropriate linguistic development and will have better results after CI [8]. They will also have a longer time window for some interventions such as drugs or gene therapies, which are currently under rapid development [9]. Through WES screening and confirmation by Sanger sequencing, we detected a gene that had not previously been reported as related to hearing: *HAS1*. *In silico* analyses predicted that the missense point variant observed in this family may damage HAS1 function and might lead to disease.

We classified the current variant (c.1082G>A; p.Cys361Tyr) according to ACMG/AMP guideline [10]. The PS4, PM2, PM6, PP2, and PP3 categories were feasible, leading to a categorization of "likely pathogenic." We also applied the ACMG criteria with the HL-EP specification [11]: the findings of PM2, PP1_strong, and PP3 also collectively indicated that this variant is "likely pathogenic." Hyaluronic acid, otherwise called hyaluronan, is an anionic non-sulfated glycosaminoglycan that composes the extracellular matrix in epithelial, cartilage, connective, and neural tissue [12,13]. Hyaluronan plays important roles in cell migration, proliferation, and differentiation through hyaluronan receptors such as CD44 or receptor for HA-mediated motility (RHAMM) [14-17], and studies have also reported that it can affect the progression of some tumors [18,19]. This molecule is synthesized in the inner surface of the plasma membrane by HAS, and one-third of the hyaluronan in the body is degraded and resynthesized every day [20]. In mammals, three *HAS* genes have been identified, showing 55%–71% sequence identity: *HAS1*, *HAS2*, and *HAS3* [21-25]. Although *HAS* isoforms bear high homology in their amino acid sequences, they are all located in different chromosomes [26] and show different enzymatic activity; *HAS1* requires a higher concentration of its substrate, uridine diphosphate N-acetylglucosamine (UDP-GlcNAc) [4,27]. The expression level of HAS1 is relatively low in many cell lines [28-31]. In mouse KO models, *Has2* seems to be the most important for general embryonic development, since *Has2* KO mice die at mid-gestation [32] whereas *Has1* or *Has3* KO mice are viable [33,34]. Although the role of HAS1 has been described in several tumors such as multiple myeloma, bladder cancer, and breast cancer [35-37], it has not yet been studied in the auditory system.

In our study, *Has1* expression was detected as early as E10.5 in the otocyst of mice and remained present throughout embryonic auditory development. It was localized in the most apical part of luminal cells. Later stages showed that this protein was localized in the SV, hair cells, and supporting cells in the greater and lesser epithelial ridges. In the neonatal stage, *Has1* expression was detected in the SV and organ of Corti hair cells, supporting cells, and some spiral ganglion cells. In adult mice, *Has1* was mainly expressed in SV marginal cells, suggesting that its role in hearing could be related to these cells.

We obtained functional hearing thresholds from the IMPC (www.mousephenotype.org). This database provided ABR data for 14-week-old *Has1* KO mice (considered young adult animals), according to IMPC protocols. The click ABR data indicated that overall hearing was similar between the *Has1* knockout and WT control animals. However, male mice showed hearing loss at low frequencies (6, 12, and 18 kHz). The hearing thresholds of female mice were similar to those of control animals. The reason for this male penetrance is still elusive. Moreover, in the family with HHL analyzed in this study, both men and women were affected and their hearing showed delayed progressive deterioration until middle age (age 40). A limitation of the IMPC ABR data is that there were only four *HAS1* KO mice (two males and two females) compared to 458 controls (228 males and 230 females). More thorough evaluations, such as with a large number of mice, hearing tests at older ages, or susceptibility to ototoxicity, seem to be needed in these mouse models.

Thus far, the role of *HAS1* in the normal auditory system or how its genetic variant causes hearing loss is not yet clear. Since our cases of HHL showed progressive hearing deterioration after adolescence, HAS1 expression at this stage seems to be im-

portant for investigating the function of this protein in the auditory system. In mice, *Has1* was especially well-expressed in the membrane of SV marginal cells after birth, suggesting a role in ion homeostasis or cochlear metabolism. The mechanism through which the p.Cys361Tyr variant can affect HAS1 functions needs to be elucidated. This variant is located in the glycosyltransferase-like family 2 domain, and it therefore might have affected the enzymatic activity. Since HAS1 is a membrane-bound protein, the variant form might have reduced binding stability. However, gnomAD reported several variants of *HAS1* without apparent phenotypes. For example, a stop gain variant (p.Ser363Ter, variant ID: 19-52217329-G-A), containing two amino acids different from that of the variant detected in the present study, has been reported in a healthy woman—albeit without a thorough presentation of her hearing levels. The effect of a truncated form versus a point variant form needs to be studied.

In conclusion, a point variant (c.1082G>A; p.Cys361Tyr) in *Has1* was observed in a family with non-syndromic late-onset progressive hearing loss with an autosomal dominant pattern. In mice, Has1 is expressed in the otocyst during embryonic development and its strongest expression occurs in SV marginal cells in the adult stage. The precise role of HAS1 in the vestibulocochlear organ needs further investigation, such as through a KO mice study. *HAS1* may be related to human HHL and is a candidate gene for future HHL genetic testing.

CONFLICT OF INTEREST

No potential conflict of interest relevant to this article was reported.

ACKNOWLEDGMENTS

This research was supported by a Basic Science Research Program grant (NRF-2014R1A1A2054755) through the National Research Foundation of Korea (NRF), funded by the Ministry of Education, Science, and Technology. It was also supported by a grant of the Korea Health Technology R&D Project through the Korea Health Industry Development Institute (KHIDI), funded by the Ministry of Health & Welfare, Republic of Korea (HR20C0021) and Chonnam National University Hospital Biomedical Research Institute grant (No. CRI16029-1).

ORCID

Alphonse Umugire https://orcid.org/0000-0001-6515-5466
Sungsu Lee https://orcid.org/0000-0002-0755-110X
Chang-Joon Lee https://orcid.org/0000-0001-5362-5360
Youngmi Choi https://orcid.org/0000-0002-4235-1082
Taekyoung Kim https://orcid.org/0000-0001-7111-3713
Hyong-Ho Cho https://orcid.org/0000-0002-1331-4039

AUTHOR CONTRIBUTIONS

Conceptualization: HHC, SL. Data curation: AU, CJL, YC, TK. Formal analysis: SL, TK. Funding acquisition: HHC. Methodology: AU, CJL, YC, TK. Project administration: HHC, SL. Validation: AU. Visualization: AU, SL. Writing–original draft: AU, SL. Writing–review & editing: SL, HHC.

SUPPLEMENTARY MATERIALS

Supplementary materials can be found online at https://doi.org/10.21053/ceo.2022.00038.

REFERENCES

1. Friedman TB, Griffith AJ. Human nonsyndromic sensorineural deafness. Annu Rev Genomics Hum Genet. 2003 Sep;4:341-402.
2. Stelma F, Bhutta MF. Non-syndromic hereditary sensorineural hearing loss: review of the genes involved. J Laryngol Otol. 2014 Jan; 128(1):13-21.
3. Torronen K, Nikunen K, Karna R, Tammi M, Tammi R, Rilla K. Tissue distribution and subcellular localization of hyaluronan synthase isoenzymes. Histochem Cell Biol. 2014 Jan;141(1):17-31.
4. Itano N, Sawai T, Yoshida M, Lenas P, Yamada Y, Imagawa M, et al. Three isoforms of mammalian hyaluronan synthases have distinct enzymatic properties. J Biol Chem. 1999 Aug;274(35):25085-92.
5. Dickinson ME, Flenniken AM, Ji X, Teboul L, Wong MD, White JK, et al. High-throughput discovery of novel developmental phenotypes. Nature. 2016 Sep;537(7621):508-14.
6. Petersen MB. Non-syndromic autosomal-dominant deafness. Clin Genet. 2002 Jul;62(1):1-13.
7. Han HM, Kwak JW, Kim HG, Lee H, Kim YC, Park E, et al. Nationwide analysis of mortality rates and related surgical procedures in hearing disability patients in South Korea. J Audiol Otol. 2020 Oct; 24(4):204-9.
8. Pattisapu P, Lindquist NR, Appelbaum EN, Silva RC, Vrabec JT, Sweeney AD. A systematic review of cochlear implant outcomes in prelingually-deafened, late-implanted patients. Otol Neurotol. 2020 Apr;41(4):444-51.
9. Wang L, Kempton JB, Brigande JV. Gene therapy in mouse models of deafness and balance dysfunction. Front Mol Neurosci. 2018 Aug 29;11:300.
10. Richards S, Aziz N, Bale S, Bick D, Das S, Gastier-Foster J, et al. Standards and guidelines for the interpretation of sequence variants: a joint consensus recommendation of the American College of Medical Genetics and Genomics and the Association for Molecular Pathology. Genet Med. 2015 May;17(5):405-24.
11. Oza AM, DiStefano MT, Hemphill SE, Cushman BJ, Grant AR, Siegert RK, et al. Expert specification of the ACMG/AMP variant interpretation guidelines for genetic hearing loss. Hum Mutat. 2018 Nov; 39(11):1593-613.
12. Holmes MW, Bayliss MT, Muir H. Hyaluronic acid in human articular cartilage: age-related changes in content and size. Biochem J. 1988

Mar;250(2):435-41.
13. Averbeck M, Gebhardt CA, Voigt S, Beilharz S, Anderegg U, Termeer CC, et al. Differential regulation of hyaluronan metabolism in the epidermal and dermal compartments of human skin by UVB irradiation. J Invest Dermatol. 2007 Mar;127(3):687-97.
14. Hall CL, Wang C, Lange LA, Turley EA. Hyaluronan and the hyaluronan receptor RHAMM promote focal adhesion turnover and transient tyrosine kinase activity. J Cell Biol. 1994 Jul;126(2):575-88.
15. Zhang S, Chang MC, Zylka D, Turley S, Harrison R, Turley EA. The hyaluronan receptor RHAMM regulates extracellular-regulated kinase. J Biol Chem. 1998 May;273(18):11342-8.
16. Knudson CB, Knudson W. Hyaluronan-binding proteins in development, tissue homeostasis, and disease. FASEB J. 1993 Oct;7(13): 1233-41.
17. Sherman L, Sleeman J, Herrlich P, Ponta H. Hyaluronate receptors: key players in growth, differentiation, migration and tumor progression. Curr Opin Cell Biol. 1994 Oct;6(5):726-33.
18. Wu RL, Sedlmeier G, Kyjacova L, Schmaus A, Philipp J, Thiele W, et al. Hyaluronic acid-CD44 interactions promote BMP4/7-dependent Id1/3 expression in melanoma cells. Sci Rep. 2018 Oct;8(1):14913.
19. Tammi MI, Oikari S, Pasonen-Seppanen S, Rilla K, Auvinen P, Tammi RH. Activated hyaluronan metabolism in the tumor matrix: causes and consequences. Matrix Biol. 2019 May;78-79:147-64.
20. Stern R. Hyaluronan catabolism: a new metabolic pathway. Eur J Cell Biol. 2004 Aug;83(7):317-25.
21. Watanabe K, Yamaguchi Y. Molecular identification of a putative human hyaluronan synthase. J Biol Chem. 1996 Sep;271(38):22945-8.
22. Itano N, Kimata K. Molecular cloning of human hyaluronan synthase. Biochem Biophys Res Commun. 1996 May;222(3):816-20.
23. Shyjan AM, Heldin P, Butcher EC, Yoshino T, Briskin MJ. Functional cloning of the cDNA for a human hyaluronan synthase. J Biol Chem. 1996 Sep;271(38):23395-9.
24. Spicer AP, Augustine ML, McDonald JA. Molecular cloning and characterization of a putative mouse hyaluronan synthase. J Biol Chem. 1996 Sep;271(38):23400-6.
25. Spicer AP, Olson JS, McDonald JA. Molecular cloning and characterization of a cDNA encoding the third putative mammalian hyaluronan synthase. J Biol Chem. 1997 Apr;272(14):8957-61.
26. Spicer AP, Seldin MF, Olsen AS, Brown N, Wells DE, Doggett NA, et al. Chromosomal localization of the human and mouse hyaluronan synthase genes. Genomics. 1997 May;41(3):493-7.
27. Rilla K, Oikari S, Jokela TA, Hyttinen JM, Karna R, Tammi RH, et al. Hyaluronan synthase 1 (HAS1) requires higher cellular UDP-GlcNAc concentration than HAS2 and HAS3. J Biol Chem. 2013 Feb;288(8): 5973-83.
28. Kultti A, Karna R, Rilla K, Nurminen P, Koli E, Makkonen KM, et al. Methyl-beta-cyclodextrin suppresses hyaluronan synthesis by down-regulation of hyaluronan synthase 2 through inhibition of Akt. J Biol Chem. 2010 Jul;285(30):22901-10.
29. Vigetti D, Genasetti A, Karousou E, Viola M, Moretto P, Clerici M, et al. Proinflammatory cytokines induce hyaluronan synthesis and monocyte adhesion in human endothelial cells through hyaluronan synthase 2 (HAS2) and the nuclear factor-kappaB (NF-kappaB) pathway. J Biol Chem. 2010 Aug;285(32):24639-45.
30. Chow G, Tauler J, Mulshine JL. Cytokines and growth factors stimulate hyaluronan production: role of hyaluronan in epithelial to mesenchymal-like transition in non-small cell lung cancer. J Biomed Biotechnol. 2010;2010:485468.
31. Akazawa Y, Sayo T, Sugiyama Y, Sato T, Akimoto N, Ito A, et al. Adiponectin resides in mouse skin and upregulates hyaluronan synthesis in dermal fibroblasts. Connect Tissue Res. 2011;52(4):322-8.
32. Camenisch TD, Spicer AP, Brehm-Gibson T, Biesterfeldt J, Augustine ML, Calabro A Jr, et al. Disruption of hyaluronan synthase-2 abrogates normal cardiac morphogenesis and hyaluronan-mediated transformation of epithelium to mesenchyme. J Clin Invest. 2000 Aug; 106(3):349-60.
33. Bai KJ, Spicer AP, Mascarenhas MM, Yu L, Ochoa CD, Garg HG, et al. The role of hyaluronan synthase 3 in ventilator-induced lung injury. Am J Respir Crit Care Med. 2005 Jul;172(1):92-8.
34. Kobayashi N, Miyoshi S, Mikami T, Koyama H, Kitazawa M, Takeoka M, et al. Hyaluronan deficiency in tumor stroma impairs macrophage trafficking and tumor neovascularization. Cancer Res. 2010 Sep; 70(18):7073-83.
35. Kriangkum J, Warkentin A, Belch AR, Pilarski LM. Alteration of introns in a hyaluronan synthase 1 (HAS1) minigene convert PremRNA [corrected] splicing to the aberrant pattern in multiple myeloma (MM): MM patients harbor similar changes. PLoS One. 2013 Jan;8(1):e53469.
36. Golshani R, Hautmann SH, Estrella V, Cohen BL, Kyle CC, Manoharan M, et al. HAS1 expression in bladder cancer and its relation to urinary HA test. Int J Cancer. 2007 Apr;120(8):1712-20.
37. Auvinen P, Rilla K, Tumelius R, Tammi M, Sironen R, Soini Y, et al. Hyaluronan synthases (HAS1-3) in stromal and malignant cells correlate with breast cancer grade and predict patient survival. Breast Cancer Res Treat. 2014 Jan;143(2):277-86.